aerospace

MDPI

Article

ANSYS Simulation of the Thermomechanical Behavior of a Large-Sized Composite Mandrel with Consideration of Viscoelasticity

Oleg Yu Smetannikov, Lyaysan Sakhabutdinova * and Gleb Ilyinykh

Perm National Research Polytechnic University, 61400 Perm, Russia; sou2009@mail.ru (O.Y.S.); ilinykh.pnipu@yandex.ru (G.I.)
* Correspondence: lyaysans@list.ru

Abstract: The article addresses the modeling of the process of manufacturing a large-sized shell, given the thermomechanical behavior and viscoelasticity of the composite mandrel. The results of the experimental identification of viscoelasticity parameters of the examined material are presented. A numerical algorithm for adapting the experimental data for the ANSYS Mechanical APDL finite element analysis package is proposed. A Prony series expansion of the relaxation kernel is used as a model for describing the material behavior. The effect of temperature on the rate of relaxation processes is taken into account through the application of a temperature-time analogy according to the Williams–Landel–Ferry formula. The selected model with the calculated parameters was implanted into the commercial package of ANSYS Mechanical APDL. Simulation of two process steps of manufacturing a large-sized product was performed: winding and heat treatment of the shell. For this purpose, the quasistatic problem of mechanics and unsteady thermal conduction under conditions of convective heat transfer were solved by the finite element method. The influence of thermomechanical behavior of the mandrel material on the normal pressure acting on the mandrel surface as a function of temperature and force factors was estimated quantitatively and qualitatively. It was found that with respect to the nonlinear behavior of the composite material, the pressure level decreases by 50% compared to the case of using models of elastic behavior. This result justifies the importance of using complex models of material behavior in studying long-term technological processes, especially those associated with high-temperature effects.

Keywords: thermoviscoelasticity; continuous winding method; mandrel; finite element modeling; prony series; Williams–Landel–Ferry shift function; sand-polymer composition

Citation: Smetannikov, O.Y.; Sakhabutdinova, L.; Ilyinykh, G. ANSYS Simulation of the Thermomechanical Behavior of a Large-Sized Composite Mandrel with Consideration of Viscoelasticity. *Aerospace* **2022**, *9*, 117. https://doi.org/10.3390/aerospace9030117

Received: 24 October 2021
Accepted: 20 December 2021
Published: 24 February 2022

1. Introduction

The aerospace industry, despite a longstanding history, remains one of the most dynamically developing and science-intensive industries. Creation of new designs and continuous improvement of already utilized engineering solutions pose new challenges to researchers. Advanced materials and technologies developed for this industrial sector have also found wide application in civil engineering. One of such technologies is the process of manufacturing high-pressure vessels from high-strength reinforcing materials by continuous wet-winding technique [1,2]. Such shells are used today not only as aircraft engine housings, but also as containers for ground transportation of flammable liquids, toxic waste, etc. [3,4]. Due to growing areas of application, the issue of safe use of such containers is especially acute. Manufacturing application of composite shell structures requires the substantiation of their strength and reliability. Due to a variety of product configurations and the complexities of the multilayer shell manufacturing technique, the assessment of their reliability is impossible without the use of modern digital models [5].

When fabricating a pressure vessel, reinforcing material is laid out along a specified trajectory on a rotating mandrel, which determines the internal geometry of the prod-

uct [6,7]. A mandrel should have a shape and size that precisely matches the shape and size of the inner surface of a filament wound product, and also effectively absorb the force and temperature effects during winding and curing of the binder. In the process of manufacturing large-sized shells, preference is given to breakable mandrels, which are conventionally fabricated of sand-polymer mixtures or low-fluidity materials. An urgent issue in meeting the requirements for reliability and durability of filament wound products is a search for models capable of describing the behavior of new materials used for manufacture of such structures. The incorporation of the results of full-scale studies of composite materials into commercial packages of finite element analysis, such as ANSYS, NASTRAN, ABAQUS and others, is also an open question.

The studies devoted to modeling of joint deformation of composite shells and polymeric mandrels are few in number. Therefore in the context of this article it is worth highlighting the contribution of some works to this area of research. The work by Shujian Li et al. [7] presents a theoretical basis for the manufacturing technology used to fabricate hat-shaped structures from carbon fiber reinforced plastic. The authors propose a multiphysics model of field interaction, which takes into account the influence of mandrel design. The influence of the mandrel on the strain state of the structure was studied by the numerical simulation and experimental modeling. The results showed that in a hat-shaped structure the effect of temperature and degree of curing on the mandrel behavior can be insignificant.

Danielle Kugler and Tess J. Moon [8] performed several experiments and multivariate regression analysis to study the influence of mandrel material, filament tow tension, cooling rate and ring thickness (as well as their interactions) on the development of various defects and their influence on the compression strength of thin and thick cylindrical structures. As a result, the authors concluded that the residual stresses were mainly influenced by the tension and thickness of the tow, although the contribution of the mandrel material should also be considered because of its effect on the waviness of the inner surface.

Of particular interest to multiseries production of pressure vessels is the work of Haiyang Du and et al. [9]. The authors presented the concept of a shape memory polymer (SMP) mandrel for manufacturing an air duct of complex geometry made by applying the composite filament winding technique. The paper describes the finite-element model used to predict the shape recovery and general deformation behavior of the structure under external pressure and temperature used for hot forming. Good agreement between the strains predicted by the finite-element model and those measured on the SMP demonstrator confirms the possibility of using a mandrel made of smart material for manufacturing composite structures with complicated or flow-through geometries.

In recent years, constructional and structural materials on the base of sand and polymer matrix have been gaining considerable popularity. Due to the abundance of such materials, their mechanical properties have been the focus of active investigation. One of such studies is the work by Aghazadeh Mohandesi J. et al. [10], in which dispersed composites were fabricated from polyethylene terephthalate wastes by reprocessing them to molten polymer and mixing with quartz sand particles in different weight ratios (5–40% of sand particles with a diameter of 0.062–0.35 mm). The composite materials were then tested in compression and three-point bending at temperatures ranging from −20 to 80 °C. The results showed that composites made from a mixture of sand and polymer matrix have the highest mechanical strength at 25 °C. This fact agrees fairly well with the results of our study, in which the maximum values of elastic modulus and tensile strength were achieved at 22 °C.

Another study [11] investigates the mechanical behavior of a mixture of polyurethane (PU) polymer and sand by performing a series of uniaxial compression (UC) and direct tensile (DT) tests for various contents of polyurethane polymer (PUC), and at different dry densities (DD) and temperatures (TP). The results show that the axial stress-strain depends on PUC, DD and TP. In particular, the fracture mode changes gradually from brittle to ductile, and the uniaxial compressive strength (UCS), secant modulus (E 50) and

ultimate tensile strength (TS) increase linearly with increasing PUC and DD at different TP. The authors obtained linear dependencies of E 50-UCS and UCS-TS) on temperature. It is shown that positive temperatures significantly increase the strength and ductility, while negative temperatures reduce the strength and the modulus.

It should be noted that Smetannikov O.Yu., the head of the study, previously took part in the development of models of thermomechanical behavior of polymeric materials undergoing glass transition and constitutive relations for viscoelastic materials under thermorelaxation transition [12,13]. As part of the work on this topic, the team of authors carried out research on the numerical simulation of the behavior of a layered composite shell, manufactured by the method of continuous winding, taking into account the viscoelastic behavior [14]. Methods for determining effective viscoelastic characteristics for an orthotropic material are proposed and substantiated in order to save computing resources.

The aim of this article is to propose a method for fast and reliable adaptation of li-mited experimental data for the implantation of a thermoviscous elastic model of the behavior of sand-polymer mixtures in the ANSYS Mechanical analysis package using the example of the technological process of winding a shell structure. The application of the technique will make it possible to quickly identify the thermomechanical properties of the material obtained experimentally, for use in creating new geometries of mandrels, or when modernizing structures manufactured using the considered type of mandrels. It is expected that taking into account the viscoelastic mechanical behavior of the mandrel material when simulating the technological process of winding and polymerization will increase the accuracy of the numerically obtained results. This will further bring us closer to creating a digital twin of the structure under study.

2. Materials and Methods

2.1. Object of the Study

The subject of the study is a sand-polymer mandrel as part of a structure that also includes a plastic shell of the "cocoon" type and technological equipment that ensures the fixation of the mandrel. The mandrel material is a mixture of sand, polyvinyl alcohol and quartz dust, the volume of which in dry matter is 1.5%. Mandrel sections are made by molding from a prepared mixture in aluminum molds at a temperature of +15 … +35 °C. The sections are then assembled together using a mounting shaft. The process of shell winding begins after fixation of the fabricated mandrel. As soon as the shell has passed through the multistage heat treatment, hot water steam is injected into the structure to break the bonds in the composite mixture. After "steaming", the residual sand and quartz are washed out of the shell. A more detailed description of the investigated design, unfortunately, is not acceptable for reasons of commercial safety. However, the methodological aspects, material constants and quantitative regularities obtained in the work are interesting for use in modeling similar technological processes for the manufacture of various structures associated with long-term temperature exposure.

Figure 1a shows a scheme of the examined system. The radius of such structures reaches 1.5 m, the total length varies by the number of central supports and can reach 10 m. As part of the development of methodological foundations, a number of test problems are solved on a simplified model in the form of a three-layer cylinder segment (Figure 1b). Since the formulated problem deals with predictive modeling of the stress-strain state of the system in the process of shell fabrication, the main focus of the study is on the experimental identification of thermomechanical parameters of the mandrel material, taking into account viscoelasticity, and their adaptation for the commercial ANSYS Mechanical APDL package.

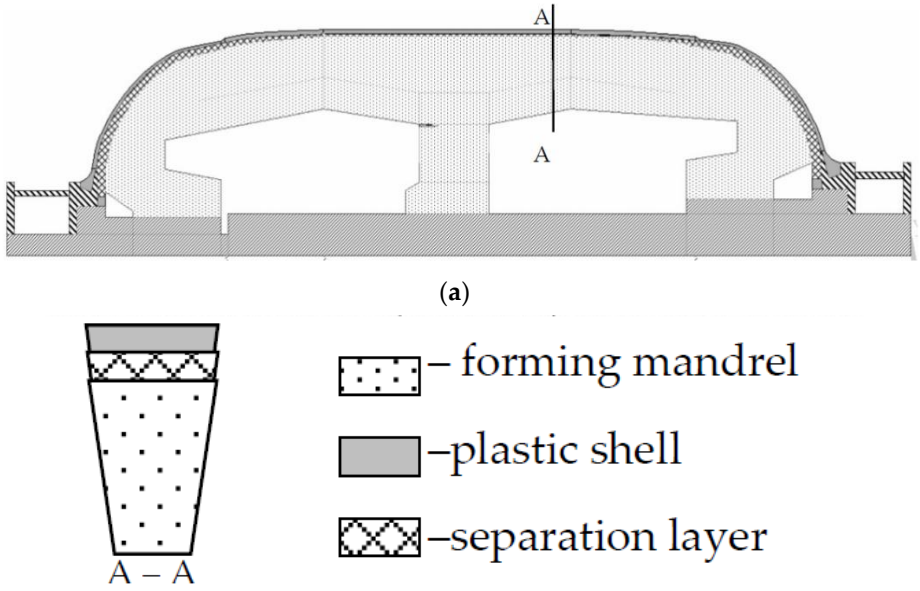

Figure 1. Computational scheme of the structure: (**a**) schematic of the real structure; (**b**) test model.

As noted above, the finished shell is subject to higher requirements for strength, reliability, and geometric accuracy. It is worth noting that the inner surface of the finished shell must not have geometric defects due to the fire and explosion hazard of the transported substances. The appearance of defects of the inner surface is affected by deformations of the mandrel in the manufacturing process. Therefore, when designing such products, it is necessary to determine the dependence of normal pressure on the surface of the mandrel on the process conditions. Russian companies often use simplified models in the elastic formulation because it is labor-intensive and requires additional financial expenses to experimentally measure contact pressure values in production. The introduction of verified numerical models makes it possible to evaluate the evolution of the normal pressure of specific points on the surface of the mandrel, as well as to illustrate for individual moments of time in the form of isofields. The development of a three-dimensional numerical analog is a new stage in improving the accuracy of calculations and numerical studies of the stress-strain state of mandrel-shell systems. Based on the peculiarities of the manufacturing process of plastic shells, calculation diagrams of the process stages are drawn. The system of external force and temperature effects is determined.

2.2. Formulation of the Simulated Problem

The general direction of research conducted by the authors of this article is the development of a numerical three-dimensional finite-element model and a program for its implementation in the commercial ANSYS Mechanical ADPL package for computation of the stress-strain state of the system composed of a sand-polymer mandrel and plastic cocoon-type shell at the stages of shell winding and polymerization under convective heating. Winding of a large-sized shell under normal conditions lasts, as a rule, for 240 h. Shell polymerization is a long multicycle process of alternating heating and cooling of the structure. Therefore, when modeling such a technological process two types of problems must be solved: the quasistatic mechanical boundary value problem, taking into account temperature deformations and the unsteady heat conduction problem under conditions of convective heat exchange with the environment in order that temperature distributions in the structure can be predicted at each moment of time.

Thus, the general statement of the problem should contain:

- Equilibrium equations:

$$\sigma_{ij,j}(\mathbf{X},t) = 0,\ \mathbf{X} \in V$$

- Physical relations:

$$\sigma_{ij}(\mathbf{X},t) = {\sigma_{ij}}^{0}(\mathbf{X},t) + \int_0^t {R'}_{ijkl}(\mathbf{X},t-\tau)d{\varepsilon^*}_{kl}(\mathbf{X},\tau),\ \mathbf{X} \in V$$

$$\varepsilon^*_{ij}(\mathbf{X},t) = \varepsilon_{ij} - \varepsilon^T_{ij}(\mathbf{X},t), \mathbf{X} \in V$$

- Geometrical relations:

$$\varepsilon_{ij}(\mathbf{X},t) = \left(u_{i,j}(\mathbf{X},t) + u_{j,i}(\mathbf{X},t)\right)/2,\ \mathbf{X} \in V$$

- Initial conditions:

$$\sigma_{ij}(\mathbf{X},0) = \sigma_0,\ \mathbf{X} \in V$$

- Boundary conditions:

$$u_i(\mathbf{X},t) = U_i(\mathbf{X},t), \mathbf{X} \in S_u$$

$$\sigma_{ij}(\mathbf{X},t) \cdot n_j = P_i, \mathbf{X} \in S_\sigma$$

where σ_{ij}, ε_{ij} are the stress and strain tensors; $\varepsilon^T_{ij}(\mathbf{X},t) = \alpha_{ij}\Delta T$ are temperature deformations, α_{ij} is the tensor of temperature expansion coefficients; $R_{ijkl}(t)$ is the tensor of relaxation functions; u_i are the components of displacement vector; ΔT is the temperature change; σ_0 are the initial stresses; U_i are the prescribed displacements on part of the boundary S_u; P_i are the surface forces prescribed on the boundary $S_\sigma (S_u \cup S_\sigma \equiv S)$.

A key point to modeling the behavior of a large-size structure is to accurately describe the thermomechanical behavior of the mandrel. Since the material of the mandrel was a composite mixture, it turned out to be possible to perform a series of full-scale tests on cylindrical samples of the mandrel material as part of the present research. Viscoelastic parameters were identified in the series of relaxation tests, in which samples were subject to compressive, tensile and torsional stresses in the temperature range from 20 to 150 °C.

2.3. Description of Experiments for Identification of Thermomechanical Parameters of Viscoelasticity for the Composite Mixture

Tests to identify the thermomechanical parameters of the composite mixture were conducted at the plant, which produces sections of forming mandrels. To accomplish this task, a series of samples with a diameter of 20 mm and a height of 60 mm were delivered to the test stand. Generally, test plans are worked out to determine all mechanical parameters, and include tension, compression and torsion tests of samples of the examined material [10,11]. However, in practice, composite mixtures based on sand and polyvinyl alcohol proved to be brittle in tension and torsion. The material samples could not withstand a full cycle of loading, so it turned to be not possible to obtain reliable strain diagrams.

Thus, further study was carried out using the results of uniaxial compression and compressive stress relaxation testing of cylindrical samples of sand-polymer mixture at normal and high temperatures.

Mechanical tests were performed on the Instron 5882 universal electromechanical system. The test system was equipped with a temperature chamber for conducting tests at temperatures from −100 °C to +350 °C, and AVE Instron non-contact video extensometer. During the tests, the accuracy of the measuring equipment had the following parameters:

- Load measurement accuracy: 0.5% of the measured value;
- Strain measurement accuracy ±2 μm.

Figure 2a presents the photos of the material sample in the chamber of testing machine. A total of 20 samples were tested at normal (22 °C) and high (70 °C, 110 °C, 150 °C) temperatures, five samples at each temperature. The samples were loaded at a constant speed of the cross bar of 1 mm/min. Figure 2c shows the characteristic deformation diagrams at 22 °C.

(**a**)

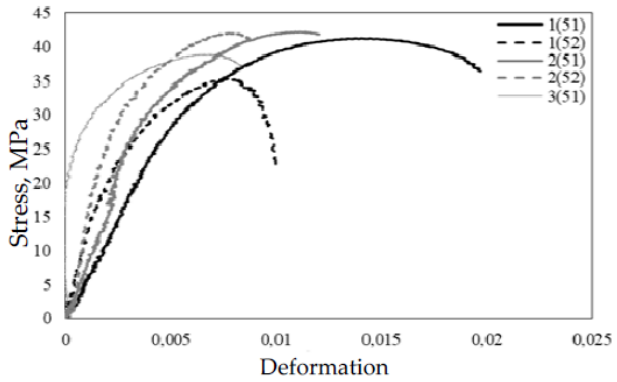

(**b**)

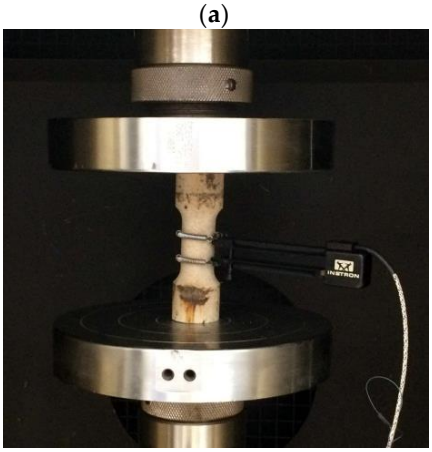

(**c**)

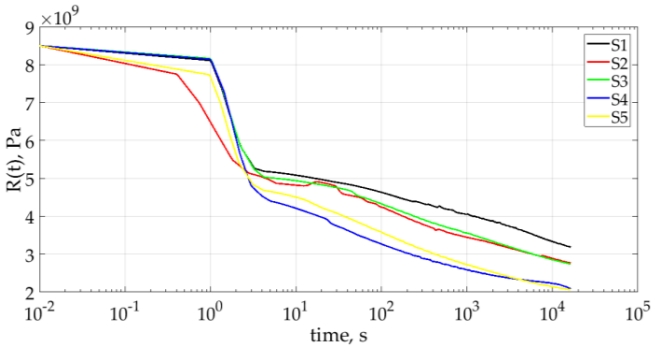

(**d**)

Figure 2. Compression testing of cylindrical samples: (**a**) with test system tooling used during tests, (**b**) compression strain diagram at 22 °C, (**c**) sample before the compression stress relaxation test, (**d**) compressive stress relaxation at 22 °C.

The photo in Figure 2b demonstrates a material sample thinned to a diameter of 15 mm in the measuring zone for compression stress relaxation test. Additionally, 20 samples were tested at temperatures similar to those used in the compression test. Testing time at 22 °C was 8 h and at 4 h high temperatures.

Before testing at high temperatures, the samples were subjected to linear heating at a rate of 10 °C per minute and thermostated at this temperature for two hours to warm up all elements of the loading system and the temperature chamber. During tests, the samples were loaded at a constant speed of the cross bar of 10 mm/min to the stress values of 30% of the static compressive strength at a given temperature. Figure 2d shows the characteristic deformation diagrams at 22 °C.

The results of compression tests of sand-polymer composition samples showed that with increasing temperature the strength properties of the material in compression decrease monotonically. For the examined samples, the decrease in strength was 78% over the entire temperature range from 22 °C to 150 °C. The stiffness properties of the material also decreased with increasing temperature. The decrease in stiffness was 80%. The stiffness properties decreased with the same intensity as the strength properties. Similar trends were observed in the relaxation tests. It was found that the value of the instantaneous modulus

at normal temperature (22 °C) is E = 9200 MPa. At increasing temperature up to 70 °C the value of modulus decreased by 33%, up to 110 °C by 76%, and up to 150 °C and by 84%. The obtained results served as the basis for constructing the hypothesis about the possibility of describing the behavior of composite mixture as a linear-viscoelastic material.

2.4. Mathematical Model for Describing the Material Behaviour

Since the initial data for the description of the material behavior were the experimental relaxation curves of the mandrel materials, the behavior can be described (according to [10]) as linear viscoelastic and thermorheological simple. In this case, as the constitutive relations it is suggested to use the Prony viscoelastic model [15–20], in which the sum of exponents with a constant bulk compression modulus is taken as the relaxation kernel:

$$\sigma_{ij}(\mathbf{X}, t) = \int_0^t 2G(t-\tau)\,\frac{de_{ij}(\mathbf{X}, \tau)}{d\tau}d\tau + \delta_{ij}K\theta(\mathbf{X}) \tag{1}$$

where e_{ij} is the strain tensor deviator, θ is the volume strain K is the volume compression modulus, $G(t)$ is the shear modulus:

$$G(t) = G_0\left[\alpha_0^G + \sum_{i=1}^{n_G}\alpha_i^G \exp\left(-\frac{t}{\tau_i^G}\right)\right] \tag{2}$$

α_i^G is relative shear modules for shear relaxation times τ_i^G, n_G is the number of shear relaxation times, from the conditions $G_0 = G|_{t=0}$, $G_\infty = G|_{t=\infty}$ it follows that:

$$\alpha_0^G = \frac{G_\infty}{G_0}\sum_{i=1}^{n_G}\alpha_i^G = \frac{G_0 - G_\infty}{G_0} \tag{3}$$

In the selected model it is assumed that the material experiences only shear relaxation at a constant value of the bulk compression modulus. The identification of parameters can be conveniently done using the uniaxial tension-compression test data. The modulus of relaxation in the case of uniaxial tension-compression has a form similar to (2):

$$E(t) = E_0\left[c_0 + \sum_{i=1}^{N_e} c_i \exp\left(-\frac{t}{\beta_i}\right)\right]$$

where c_i are the relative tensile-compressive modules for the relaxation times β_i, N_e is the number of expansion-compression relaxation times.

By analogy with (3), from $E_0 = E|_{t=0}$, $E_\infty = E|_{t=\infty}$ we get the following:

$$c_0 = \frac{E_\infty}{E_0},\ \sum_{i=1}^{N_e} c_i = \frac{E_0 - E_\infty}{E_0} \tag{4}$$

We assume that the number of relaxation times for shear (τ_i^G) is equal to that of tension-compression (β_i) and is expressed as $N_e = n_G = n$. Then from (3) and (4) we can obtain the following relation:

$$\sum_{i=1}^{n}\alpha_i^G = \sum_{i=1}^{n} c_i\left[\frac{G_0 - G_\infty}{G_0}\cdot\frac{E_0}{E_0 - E_\infty}\right]$$

Specifically, $B = \frac{G_0 - G_\infty}{G_0}\cdot\frac{E_0}{E_0 - E_\infty}$, we get

$$\alpha_i^G = c_i \cdot B \tag{5}$$

It is known that

$$G_0 = \frac{E_0}{2(1+\nu_0)} \tag{6}$$

$$G_\infty = \frac{E_\infty}{2(1+\nu_\infty)} \tag{7}$$

ν_0, ν_∞ are the values of the Poisson's ratio at time $t = 0$ and $t = \infty$, respectively. The value ν_∞ is found from the condition of constancy of the bulk elastic modulus:

$$K^* = \frac{E_0}{3(1-2\nu_0)} = const \tag{8}$$

$$K_\infty = K^* = \frac{E_\infty}{3(1-2\nu_\infty)} \Rightarrow \nu_\infty = 0.5\left(1 - \frac{E_\infty}{3K^*}\right) \tag{9}$$

Substituting (9) into (7), yields:

$$G_\infty = \frac{E_\infty}{2\left(1+0.5\left(1-\frac{E_\infty}{3K^*}\right)\right)} = E_\infty \frac{3}{9-\frac{E_\infty}{K^*}} \tag{10}$$

Thus, from (5), (6), (8) and (10) it is possible to calculate α_i^G, K^*, G_0, G_∞ by finding beforehand c_i, E_0, E_∞, ν_0. from the tensile-compression experiment. For this purpose the constitutive relations for the uniaxial case were used:

$$\sigma(t) = \int_0^t \left[E_\infty + E_0 \sum_{i=1}^{N_e} c_i \exp\left(-\frac{t-\tau}{\beta_i'}\right)\right] d\varepsilon(\tau) \tag{11}$$

where $\beta_i' = \frac{\beta_i}{A(T)}$ is the reduced time, $A(T)$ is the shift function. The material is assumed to be thermo-realistically simple, so the Williams–Landel–Ferry shift function is used [21–24]:

$$\log(A(T)) = \frac{C_1(T-T_r)}{C_2 + (T-T_r)} \tag{12}$$

where $\log(A(T))$ is the decadic logarithm of the shift function, T is the current temperature, T_r is the base temperature constant, C_1, C_2 are the empirical constants for the material.

In the ANSYS Mechanical APDL environment, the selected mechanical behavior of materials can be described by means of the Prony model. The parameters of this model c_i, β_i are the approximation coefficients of the generalized relaxation function (1).

The influence of temperature on the rate of relaxation processes can be taken into account by means of the Shift model (referred in the literature as the Williams–Landel–Ferry shift function) with the parameters of the Williams–Landel–Ferry model (12). The parameters of the temperature-time shift factor are determined by solving the system of linear algebraic equations derived from a comparison of the relaxation curves at three different temperatures.

$$\begin{bmatrix} T_1 - Tb; & -\left\langle \log\left(\frac{\overline{\beta}_{i1}}{\beta_i}\right)\right\rangle \\ T_2 - Tb; & -\left\langle \log\left(\frac{\overline{\beta}_{i2}}{\beta_i}\right)\right\rangle \end{bmatrix} \cdot \begin{Bmatrix} C_1 \\ C_2 \end{Bmatrix} = \begin{Bmatrix} (T_1 - T_b) \cdot \left\langle \log\left(\frac{\overline{\beta}_{i1}}{\beta_i}\right)\right\rangle \\ (T_2 - T_b) \cdot \left\langle \log\left(\frac{\overline{\beta}_{i2}}{\beta_i}\right)\right\rangle \end{Bmatrix} \tag{13}$$

The approximation coefficients (4) are determined by minimizing the mean square discrepancy:

$$\sum_j \left(E_0\left[\frac{E_\infty}{E_0} + \sum_{i=1}^{N_e} c_i \exp\left(-\frac{t_j}{\beta_i}\right)\right] - E_B(t_j)\right)^2 = \min \tag{14}$$

Thus, the general algorithm of the methodology for adapting experimental data can be implemented through the following steps:

(1) Recalculation of experimental curves of the material samples to material relaxation function curves at different temperatures;
(2) Averaging of the relaxation function curves at each temperature;
(3) Calculation of the temperature-time shift parameters (13);
(4) Calculation of the approximation coefficients (14).

This algorithm was first implemented using the computational Matlab package. A console-based application was then written in Python to automate the proposed approach. This utility program will allow further rapid processing of experimental data for sand-polymer mixtures with other components. One of the applications was processing of test data obtained from testing the original composition with and without increased amounts of silica dust.

2.5. Processing of Test Results of Testing CPS Samples

The selected formulation of the material behavior model and the algorithm proposed in Section 2.4 were used to process the material relaxation curves obtained by experiment at the specified temperatures. The results of processing the data of compressive stress relaxation tests of mixture samples are shown in Figure 3. A generalized diagram of the relaxation function curves for specified temperatures is shown in Figure 3a. Generalized curves of the relaxation function and the functions obtained with aid of time-temperature shifting are shown in Figure 3b.

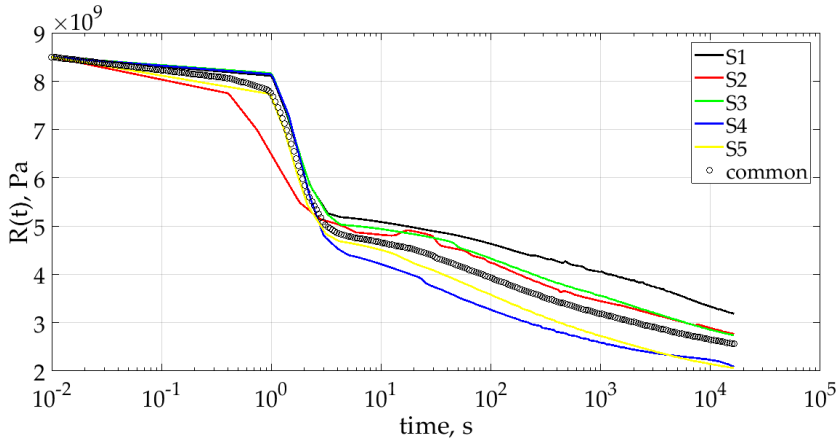

(**a**)

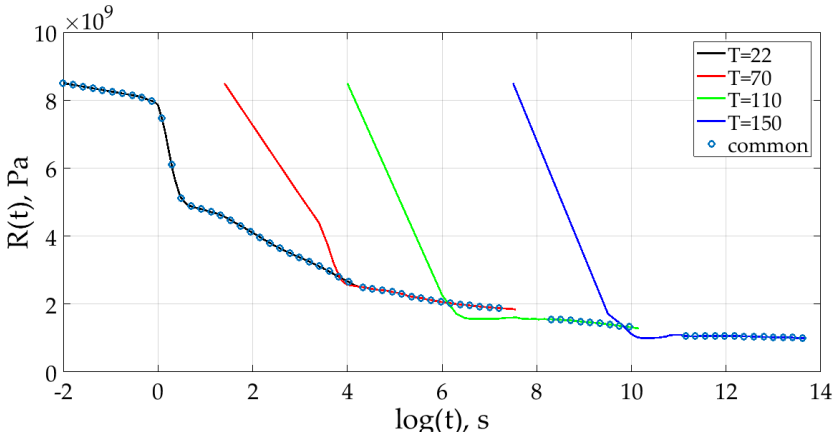

(**b**)

Figure 3. Relaxation function curves: (**a**) samples at 22 °C; (**b**) result of temperature-time shifting. Thin line—experiment, marker—result of averaging.

After processing the experimental data by the methods of nonlinear programming, we obtained the following values of the material model (11) constants for $N_e = 20$, satisfying the condition of minimum discrepancy (14) between the experimental and calculated data:

- Modules $E_0 = 8.5$ GPa, $E_\infty = 0.992$ GPa;
- Constants of the temperature-time shift function Equation (12) $T_b = 295$ K, $C_1 = 65.8$, $C_2 = 876$ K.

The maximum relative discrepancy of the numerical calculation did not exceed 10%. The distribution of the weight coefficients c_i over the relaxation times β_i is shown in Table 1.

Table 1. The values of approximation coefficients of the generalized relaxation function for the mandrel material.

i	β_i	c_i	i	β_i	c_i
1	1.0000×10^{-2}	5.2051×10^{-3}	11	1.6967×10^{6}	5.6394×10^{-3}
2	6.6521×10^{-2}	1.7096×10^{-6}	12	1.1287×10^{7}	2.1466×10^{-2}
3	4.4251×10^{-1}	9.2538×10^{-2}	13	7.5081×10^{7}	3.3812×10^{-2}
4	2.9436	2.3663×10^{-1}	14	4.9945×10^{8}	7.2477×10^{-3}
5	1.9581×10^{1}	1.0725×10^{-1}	15	3.3224×10^{9}	1.3033×10^{-2}
6	1.3026×10^{2}	1.2601×10^{-1}	16	2.2101×10^{10}	2.9735×10^{-2}
7	8.6650×10^{2}	6.6580×10^{-2}	17	1.4702×10^{11}	6.5812×10^{-3}
8	5.7640×10^{3}	3.1081×10^{-2}	18	9.7800×10^{11}	6.1872×10^{-3}
9	3.8343×10^{4}	5.2300×10^{-2}	19	6.5058×10^{12}	4.0132×10^{-3}
10	2.5506×10^{5}	3.6561×10^{-2}	20	4.3277×10^{13}	1.3420×10^{-3}

The validation of the proposed method for describing the behavior of the composite mixture was done by applying the inverse procedure. The kernel relaxation curves at given temperatures were constructed using the obtained weight coefficients and constants of the Williams-Landel-Ferry function. The results of this stage are shown in Figure 4 in the form of experimental and calculated relaxation curves.

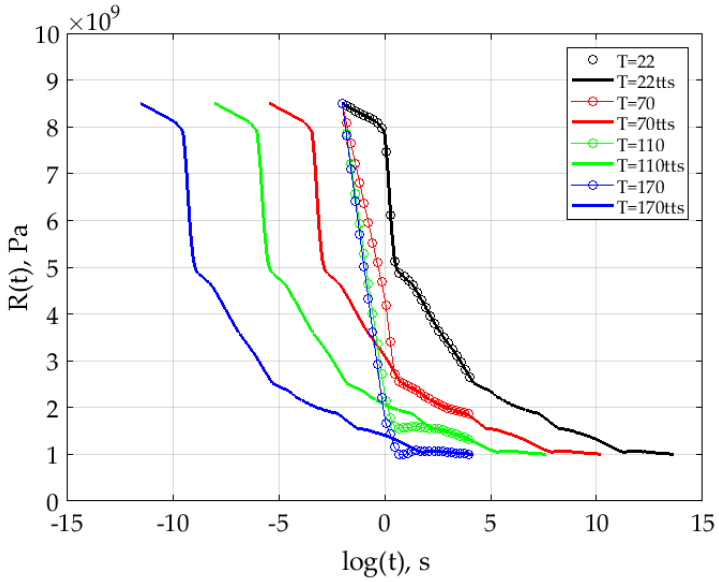

Figure 4. Convergence of the generalized relaxation curve and calculated relaxation curves. Bold lines (tts)—calculated relaxation function curves; lines with markers—original relaxation function curves. Black curves for temperature 22 °C, red curves for temperature 70 °C, green curves for temperature 110 °C, blue curves for temperature 170 °C.

From the analysis of Figure 4 it follows that with the reverse temperature-time shift, the average relaxation curve coincides with the initial one, which corresponds to the proposed method. At temperatures other than 22 °C, it is shown that the instantaneous characteristics diverge significantly at time close to 0. Starting from 10^1 s, the initial and calculated curves are identical. Since the processes considered in this paper are long, about 10^6–10^8 s, the results obtained can be used to solve engineering problems.

2.6. Numerical Model in ANSYS Mechanical APDL

The numerical model is built in ANSYS Mechanical APDL. A representative structure volume in the form of a three-layer cylinder segment is considered in order to save computing resources for research. Plane182 finite elements were used for constructing two-dimensional geometry, Solid185 used for the three-dimensional problem of the stress-strain state and Solid30 for calculating the temperature fields. Periodic boundary conditions are set at the nodes of the cut faces:

$$U_z(\mathbf{x})|_{\mathbf{x}\in S_2} = U_z(\mathbf{x})|_{\mathbf{x}\in S_4}$$
$$U_\Phi(\mathbf{x})|_{\mathbf{x}\in S_3} = U_\Phi(\mathbf{x})|_{\mathbf{x}\in S_5}$$

where U_z, U_Φ—axial and angular node displacements; S_2, S_3, S_4, S_5—side surfaces of finite-element analogue. The forces produced in structure when high-modulus reinforcing tapes are pulled onto a forming mandrel. To determine these forces, separate layers were combined into one layer with effective characteristics and effective initial stresses, which provide the necessary level of pressure from the shell to the mandrel. More details about the possibility of such an approach are described in our work [14]. The transfer of pressure from the laying of layers to the surface of the mandrel is ensured by the coupled mesh, in other words, common nodes are located at the boundaries of different materials.

When solving the problem of unsteady thermal conductivity, an initial temperature of 23 °C was set. A surface load of the 'conv' type was introduced on the outer free surface S_1 (Figure 5a), providing heat transfer from the environment with the surface temperature T_{env} with a convection film coefficient α. The solution to the problem is organized in two stages. At the first stage, the boundary value problem of unsteady heat conduction is solved. At the second stage in the cycle for successive moments of time, the boundary thermoviscoelastic problem is solved, in which the temperature fields corresponding in time, obtained at the first stage, act as volumetric loads.

The estimation of the dependence of the magnitude of the normal pressure between the separating layer and the mandrel at the stage of winding on the size of the elements is carried out. The number of nodal unknowns varied by the number of elements along the side faces, as well as by the thickness. The dependence of normal pressure on the number of nodal unknowns is shown in Figure 4b. The convergence was evaluated on elastic models of material. Then, for the structure model, an analysis of the temperature change on the shell surface and on the mandrel surface during heat treatment was carried out. Thermometry values were compared in the production of a real product with the results of numerical simulations (Figure 4c). From the diagrams obtained, it was concluded that for further research, it would be sufficient to divide into 10 elements along the side faces, 30 in the thickness of the mandrel, five in the thickness of the separating layer and 15–20 in the thickness of the shell. The results of modeling the problem of thermal conductivity correspond to the results of thermometry of a real structure, which indicates the correctness of the selected material constants, as well as the coefficients of convective heat transfer.

It is noticed that the value of the normal pressure is significantly affected by the number of elements in the shell and the separating layer. However, when considering a model of a real structure, such a number of partitions leads to a significant increase in the duration of computations, which is undesirable when solving typical technical (engineering) problems. Therefore, the results of modeling a real structure are outside the scope of this article and require a separate extensive analysis from the standpoint of rationalizing the finite element mesh and approaches to taking into account external force factors.

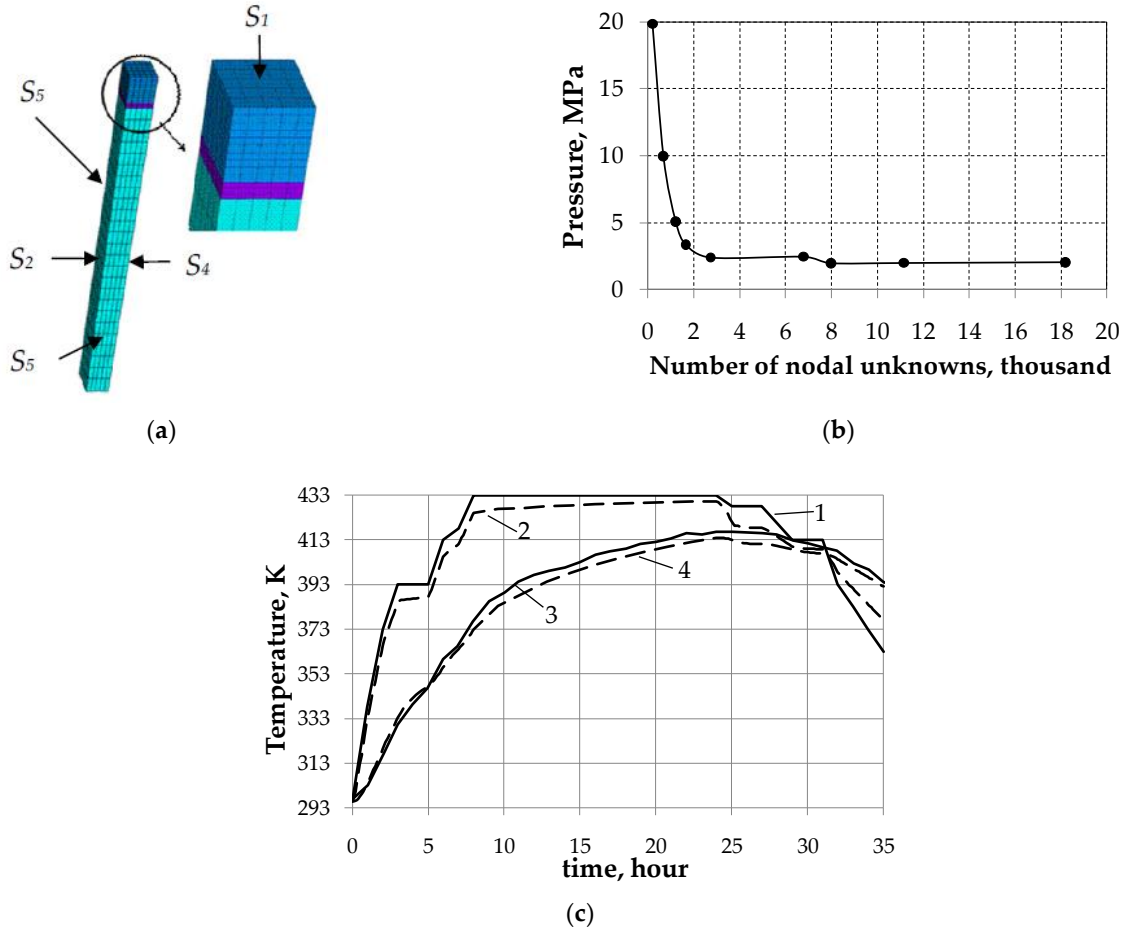

Figure 5. Convergence of the generalized relaxation curve and calculated relaxation curves. Thin lines—calculated relaxation function curves; bold lines—original relaxation function curves. (**a**) Finite element analogue with boundaries specification; (**b**) dependence of the pressure on the surface of the mandrel at the end of the winding on the number of nodal unknowns; (**c**) temperature versus time at separate points: 1—ambient temperature, 2—calculated temperature on the surface of the shell, 3—real temperature on the surface of the mandrel, 4—calculated temperature on the surface of the mandrel.

3. Results

The model proposed in this study to describe the behavior of the material of a forming mandrel was used for numerical simulation of the shell manufacturing process using as an example the test model depicted in Figure 1b. To this end, three problems were solved sequentially. First, based on the results of numerical calculations the evolution of the stress-strain state of the structure at the winding stage was predicted. The multilayer shell winding process was simulated as a single-stage build-up of the shell thickness with distributed initial forces. At the second stage, the evolution of temperature fields in the structure during polymerization of the shell binder was determined. Finally, at the third stage, the evolution of the stress-strain state of the system was calculated taking into account temperature deformation during polymerization.

The dependence of the simulated mandrel material behavior on the stress-strain state of the structure was evaluated by considering changes in the normal pressure on mandrel surface during the whole technological process. Figure 6 shows the results for the elastic and thermo-viscoelastic models of material behavior.

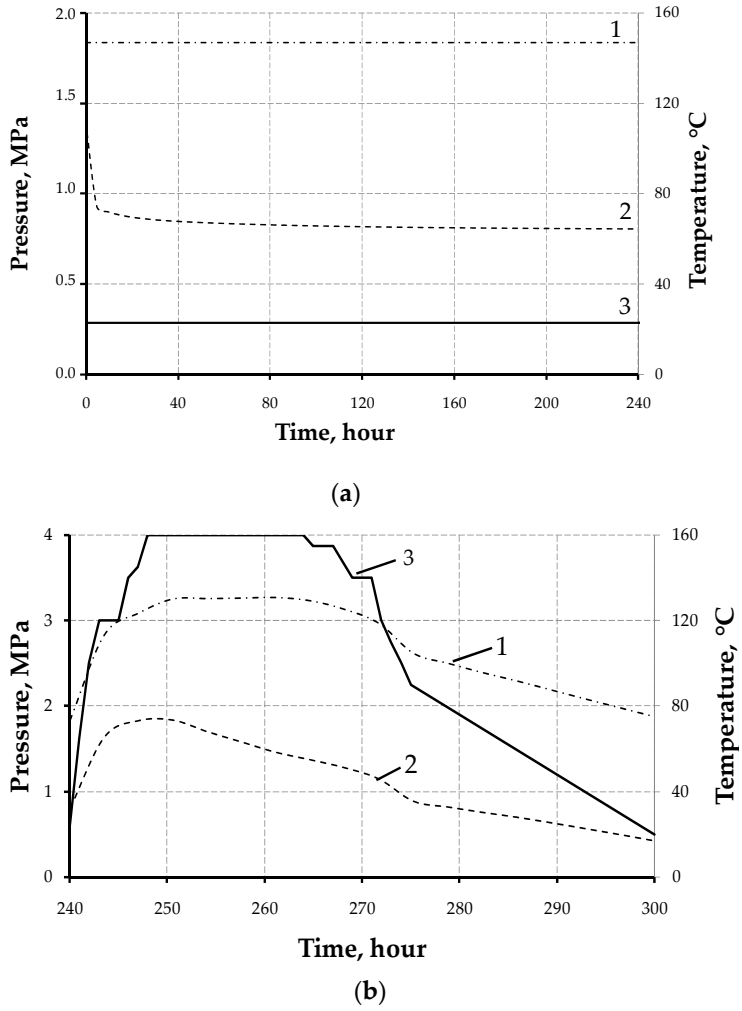

Figure 6. Comparison of the evolution of the normal pressure on the mandrel surface: (**a**) winding stage, (**b**) polymerization stage. 1—Elastic model of mandrel material behavior; 2—thermo-viscoelastic model of mandrel material behavior; 3—temperature regime.

A comparison of the normal pressure dynamics during the winding step is shown in Figure 6a, for the polymerization step in Figure 6b. For the elastic model, at the first stage, the pressure on the mandrel surface was 1.84 MPa, at the second stage, the maximum pressure reached 3.27 MPa, then decreased to 1.88 MPa. In the viscoelastic formulation, at the first stage, the pressure decreased from 1.39 MPa to 0.8 MPa; at the second stage, the maximum value was 1.84 MPa and decreased to 0.4 MPa.

For the elastic model, the pressure values are on average 1 MPa higher than for the viscoelastic one. The difference in the value of the pressure on the surface of the mandrel is 50-70% between the two models of mandrel behavior. The obtained result emphasizes the importance of creating improved models when simulating long-term technological processes at elevated temperatures.

For a model of a real structure, a similar comparison has not yet been made, because it requires accuracy in the introduction of integral estimates. Currently, work in this direction is underway.

4. Discussion

At the moment, there are many studies devoted to the description of the thermo-mechanical and viscoelastic behavior of various materials. Scientists are proposing new models based on classical models to describe the behavior of new materials, such as smart materials. In a number of works, new constitutive relations are formulated that take

into account the contribution of thermal relaxation and phase transitions to the history of deformation [25–27]. An inevitable consequence of the refinement of the description of properties in such models is the complexity of their application in solving real technological problems, associated, first of all, with significant computational costs.

Most of the mentioned works are devoted to the study of the properties of polymers and composites based on them, which are part of finished products. In this study, we investigated the material of auxiliary equipment—a mandrel, which is a special sand-polymer water-soluble mixture. The thermomechanical behavior of this class of materials is described mainly at the level of the temperature dependence of Young's modulus and ultimate strength. Thus, to refine the calculation of the stress-strain state of the mandrel-cocoon system, it is necessary to select an adequate physical model suitable for implantation into commercial CAE programs, as well as a methodology for its experimental provision.

Based on the foregoing, the authors chose the Prony linear-viscoelastic model as the most adequate thermomechanical model of the behavior of the mandrel material, taking into account the hypothesis of the thermorheologically simple behavior of the sand-polymer mixture. ANSYS provides the ability to introduce separate functions to describe bulk and shear relaxation. To identify a model that takes into account bulk relaxation, in addition to uniaxial tension (compression), shear (torsion) tests at several heating levels are required. However, attempts to measure torsional relaxation with existing equipment have yielded unsatisfactory errors. As a result, it was decided to introduce the hypothesis of constancy of the bulk modulus. As a result of the analysis of the similarity of the relaxation curves at different temperatures, it was concluded that the hypothesis of the temperature-time shift in the Williams–Landel–Ferry form, which provided a satisfactory combination of the local relaxation curves into a generalized curve, was concluded.

The article proposes an algorithm for adapting experimental data for implantation into the applied commercial package ANSYS Mechanical APDL. All the key stages of adaptation are illustrated in Figures 2–4. The values of the obtained mechanical constants for the sand-polymer mixture, as well as the values of the expansion constants of the modulus in the Prony series, are given. The authors carried out a quantitative estimation of the influence of thermomechanical behavior, taking into account the viscoelasticity of the mandrel material, on the evolution of normal pressure on its surface.

The novelty of the results obtained is due to the fact that at present most of the works are devoted to modeling the winding on metal mandrels [28,29] and devices [30,31], while the authors note that even in this case, to determine the stress level in structures, winding is required take into account, in particular, the nonlinear behavior of aluminum [32,33].

The use of polymer sand mixtures in the production leads to a reduction in the cost of the technological process for the manufacture of shells using various mandrels. As a result, active studies of the properties of such materials and a description of their behavior begin [7,10,11,30]. In this vein, our proposed approach to adapting experimental data for existing models of thermomechanical behavior in the ANSYS Mechanical package will be useful for engineers and researchers involved in numerical modeling of the manufacture of structures based on polymer mandrels.

The use of nonlinear models to describe the mandrel, which in the structure can occupy up to 90% of the volume, will significantly increase the accuracy of the results of numerical modeling of the stress-strain state of the structure.

In the future, refined numerical models will optimize the technological process of manufacturing shells by the winding method [29,32] and improve the configuration of the forming mandrel.

5. Conclusions

The article presents a mathematical statement of the problems of deformable solid mechanics for modeling the technological process of manufacturing large-sized shells by the method of continuous wet winding. The possibility of describing the experimental

relaxation curves of the mandrel material by the constitutive relations of the viscoelastic Prony model with a constant bulk compression modulus has been justified mathematically.

The results of the main stages of adaptation of experimental curves for use in the commercial package ANSYS Mechanical APDL are illustrated. The following material parameters were obtained for the considered sand-polymer mixture:

- Modules 8.5 GPa, 0.992 GPa;
- Constants of the temperature-time shift function T_b = 295 K, C_1 = 65.8, C_2 = 876 K.

Then, using the example of a multilayer cylinder segment, the influence of the model of the mandrel material on the dependence of the normal pressure at the interface between the heat-shielding layer and the mandrel was estimated. In the numerical analysis of the technological process, it was found that for the elastic model at the winding stage, the maximum pressure on the mandrel surface is 1.84 MPa, at the heat treatment stage −3.27 MPa, followed by a decrease to 1.88 MPa. In the viscoelastic formulation, at the first stage, relaxation decreases the pressure from 1.39 MPa at the end of winding to 0.8 MPa by the time of the start of heat treatment. During the second stage, the maximum value was 1.84 MPa, and the minimum −0.4 MPa. Thus, the discrepancy between the elastic and viscoelastic behavior of the material gives an average of 50–70% throughout the entire process.

It is important to note that the decrease in the pressure value under normal conditions is commensurate with the change in the value of the relaxation core of the mandrel material at a temperature of 22 °C. These data indicate the correspondence of the numerical model to real processes occurring in the material.

The results of the main stages of adaptation of experimental curves for use in the commercial package ANSYS Mechanical APDL are illustrated. For the considered sand-polymer mixture, the following material parameters were obtained.

Author Contributions: Conceptualization, O.Y.S.; methodology, O.Y.S.; software, L.S., G.I.; validation, L.S. and G.I.; writing—original draft preparation, O.Y.S., L.S. and G.I.; writing—review and editing, O.Y.S., L.S. and G.I.; visualization, L.S.; funding acquisition, O.Y.S. All authors have read and agreed to the published version of the manuscript.

Funding: O.Y.S., L.S. and G.I. acknowledge the financial support of the Ministry of Science and Higher Education of the Russian Federation in the framework of the program of activities of the Perm Scientific and Educational Center "Rational Subsoil Use".

Institutional Review Board Statement: Not applicable.

Informed Consent Statement: Not applicable.

Data Availability Statement: Not applicable.

Conflicts of Interest: The authors declare no conflict of interest.

References

1. Zhang, B.; Xu, H.; Zu, L.; Li, D.; Zi, B.; Zhang, B. Design of filament-wound composite elbows based on non-geodesic trajectories. *Compos. Struct.* **2018**, *189*, 635–640. [CrossRef]
2. Sebaey, T.A. Design of Oil and Gas Composite Pipes for Energy Production. *Energy Procedia* **2019**, *162*, 146–155. [CrossRef]
3. Kim, C.-U.; Song, J.-I. Development of lightweight fiber-reinforced composite pins for heavy load long pitch roller chains. *Compos. Struct.* **2019**, *236*, 111839. [CrossRef]
4. Lai, C.; Hu, Y.; Zheng, Q.; Fan, H. All-composite flanges for anisogrid lattice-core sandwich panels to bear stretching load. *Compos. Commun.* **2020**, *19*, 189–193. [CrossRef]
5. Kordkheili, S.H.; Khorasani, R. On the geometrically nonlinear analysis of sandwich shells with viscoelastic core: A layerwise dynamic finite element formulation. *Compos. Struct.* **2019**, *230*, 111388. [CrossRef]
6. Fu, J.; Yun, J.; Jung, Y.; Lee, D. Generation of filament-winding paths for complex axisymmetric shapes based on the principal stress field. *Compos. Struct.* **2017**, *161*, 330–339. [CrossRef]
7. Li, S.; Zhan, L.; Chang, T. Numerical simulation and experimental studies of mandrel effect on flow-compaction behavior of CFRP hat-shaped structure during curing process. *Arch. Civ. Mech. Eng.* **2018**, *18*, 1386–1400. [CrossRef]

8. Kugler, D.; Moon, T.J. The effects of Mandrel material and tow tension on defects and compressive strength of hoop-wound, on-line consolidated, composite rings. *Compos. Part A Appl. Sci. Manuf.* **2002**, *33*, 861–876. [CrossRef]
9. Du, H.; Liu, L.; Leng, J.; Peng, H.-X.; Scarpa, F.; Liu, Y. Shape memory polymer S-shaped mandrel for composite air duct manufacturing. *Compos. Struct.* **2015**, *133*, 930–938. [CrossRef]
10. Mohandesi, J.A.; Refahi, A.; Meresht, E.S.; Berenji, S. Effect of temperature and particle weight fraction on mechanical and micromechanical properties of sand-polyethylene terephthalate composites: A laboratory and discrete element method study. *Compos. Part B Eng.* **2011**, *42*, 1461–1467. [CrossRef]
11. Bai, Y.; Liu, J.; Cui, Y.; Shi, X.; Song, Z.; Qi, C. Mechanical behavior of polymer stabilized sand under different temperatures. *Constr. Build. Mater.* **2021**, *290*, 123237. [CrossRef]
12. Matveenko, V.P.; Smetannikov, O.; Trufanov, N.A.; Shardakov, I.N. Models of thermomechanical behavior of polymeric materials undergoing glass transition. *Acta Mech.* **2012**, *223*, 1261–1284. [CrossRef]
13. Matveenko, V.; Smetannikov, O.Y.; Trufanov, N.A.; Shardakov, I.N. Constitutive relations for viscoelastic materials under thermorelaxation transition. *Acta Mech.* **2015**, *226*, 2177–2194. [CrossRef]
14. Sahabutdinova, L.R.; Smetannikov, O.Y.; Ilinyh, G.V. Numerical simulation of the process manufacture of large-scale composite shell taking into account thermo viscoelastic. *Tomsk. State Univ. J. Math. Mech.* 2022, *in press*.
15. Mauro, J.C.; Mauro, Y.Z. On the Prony series representation of stretched exponential relaxation. *Phys. A Stat. Mech. Its Appl.* **2018**, *506*, 75–87. [CrossRef]
16. Luo, R.; Lv, H.; Liu, H. Development of Prony series models based on continuous relaxation spectrums for relaxation moduli determined using creep tests. *Constr. Build. Mater.* **2018**, *168*, 758–770. [CrossRef]
17. Li, L.; Li, W.; Wang, H.; Zhao, J.; Wang, Z.; Dong, M.; Han, D. Investigation of Prony series model related asphalt mixture properties under different confining pressures. *Constr. Build. Mater.* **2018**, *166*, 147–157. [CrossRef]
18. Parka, S.W.; Schapery, R.A. Methods of interconversion between linear viscoelastic material functions. Part I—A numerical method based on Prony series. *Int. J. Solids Struct.* **1999**, *36*, 1653–1675. [CrossRef]
19. Brinson, L.C.; Lin, W.S. Comparison of micromechanics methods for effective properties of multiphase viscoelastic composites. *Compos. Struct.* **1998**, *41*, 353–367. [CrossRef]
20. Rajan, S.; Sutton, M.A.; Fuerte, R.; Emri, I. Time temperature superposition and prony series coefficients of asphalt roof shingle material from viscoelastic creep testing. In *Challenges in Mechanics of Time Dependent Materials*; Springer: Cham, Switzerland, 2018; Volume 2.
21. Williams, M.L.; Landel, R.F.; Ferry, J.D. The Temperature Dependence of Relaxation Mechanisms in Amorphous Polymers and Other Glass-Forming Liquids. *J. Am. Chem. Soc.* **1955**, *77*, 3701–3707. [CrossRef]
22. Shim, W.; Jang, J.; Choi, J.-H.; Cho, J.-M.; Yoon, S.-J.; Choi, C.-H.; Yu, W.-R. Simulating rate- and temperature-dependent behaviors of adhesives using a nonlinear viscoelastic model. *Mech. Mater.* **2020**, *147*, 103446. [CrossRef]
23. Walubita, L.F.; Alvarez, A.E.; Simate, G.S. Evaluating and comparing different methods and models for generating relaxation modulus master-curves for asphalt mixes. *Constr. Build. Mater.* **2011**, *25*, 2619–2626. [CrossRef]
24. Vestena, P.M.; Schuster, S.L.; de Almeida, P.O.B., Jr.; Faccin, C.; Specht, L.P.; da Silva Pereira, D. Dynamic modulus master curve construction of asphalt mixtures: Error analysis in different models and field scenarios. *Constr. Build. Mater.* **2021**, *301*, 124343. [CrossRef]
25. Spathis, G.; Kontou, E. Rheological constitutive equations for glassy polymers, based on trap phenomenology. *Mech. Time-Depend. Mater.* **2018**, *24*, 73–83. [CrossRef]
26. Barth, N.; George, D.; Ahzi, S.; Remond, Y.; Joulaee, N.; Khaleel, M.A.; Bouyer, F. Simulation of cooling and solidification of three-dimensional bulk borosilicate glass: Effect of structural relaxations. *Mech. Time-Depend. Mater.* **2013**, *18*, 81–96. [CrossRef]
27. Annarasa, V.; Popov, A.A.; De Focatiis, D.S.A. A phenomenological constitutive model for the viscoelastic deformation of elastomers. *Mech. Time-Depend. Mater.* **2020**, *24*, 463–479. [CrossRef]
28. Yang, H.; Luo, X.; Shen, K.; Yuan, Y.; Fu, Q.; Gao, X.; Jiang, L. The role of mandrel rotation speed on morphology and mechanical properties of polyethylene pipes produced by rotational shear. *Polymer* **2019**, *184*, 121915. [CrossRef]
29. Liu, C.; Shi, Y. Design optimization for filament wound cylindrical composite internal pressure vessels considering process-induced residual stresses. *Compos. Struct.* **2020**, *235*, 111755. [CrossRef]
30. Endo, V.T.; Pereira, J.C.D.C. Linear orthotropic viscoelasticity model for fiber reinforced thermoplastic material based on Prony series. *Mech. Time-Depend. Mater.* **2017**, *21*, 199–221. [CrossRef]
31. Otero, J.A.; Rodríguez-Ramos, R.; Guinovart-Díaz, R.; Cruz-González, O.L.; Sabina, F.J.; Berger, H.; Böhlke, T. Asymptotic and numerical homogenization methods applied to fibrous viscoelastic composites using Prony's series. *Acta Mech.* **2020**, *231*, 2761–2771. [CrossRef]
32. Man, R.; Kim, S.; Son, C.; Kim, Y.; Jung, Y. Filament winding pattern generation for non-axisymmetric mandrels based on uniform quadrilateral elements. *J. Compos. Mater.* **2021**, *55*, 1217–1230. [CrossRef]
33. Huang, X.; Wang, B.; Lin, J.; Zhu, C. Effect of mandrel diameter on non-circularity of hollow shafts in cross wedge rolling. *Procedia Eng.* **2017**, *207*, 2376–2381. [CrossRef]